Thermal Stresses Near the Crystal-Melt Interface During the Floating-Zone Growth of CdTe Under Microgravity Environment

Kyu-Jung Lee*1

미세중력장 CdTe 플로우팅존 생성에서 결정체-용융액 계면주위의 열응력

이 규 정

A numerical analysis of thermal stress over temperature variations near the crystal-melt interface is carried out for a floating-zone growth of Cadmium Telluride (CdTe). Thermocapillary convection determines crystal-melt interfacial shape and signature of temperature in the crystal. Large temperature gradients near the crystal-melt interface yield excessive thermal stresses in a crystal, which affect the dislocations of the crystal. Based on the assumption that the crystal is elastic and isotropic, thermal stresses in a crystal are computed and the effects of operating conditions are investigated. The results show that the extreme thermal stresses are concentrated near the interface of a crystal and the radial and the tangential stresses are the dominant ones. Concentrated heating profile increases the stresses within the crystal, otherwise, the pulling rate decreases the stresses.

Key Words: 열응력(thermal stress), 플로우팅존(Floating-Zone), 열모세관대류(Thermocapillary convection), 카드뮴테룰라이드(CdTe), 미세중력장(microgravity environment),

Nomenclature

C_p: specific heat at constant pressure
E: modulus of elasticity in tension and compression
G: modulus of rigidity
e: heating extent
k: thermal conductivity
R_0: rod radius
T: temperature
u, u: displacements
V_t: pulling rate
ΔH: latent heat
ΔT: temperature difference
α: Coefficient of thermal expansion
$\bar{\alpha}$: thermal diffusivity
μ: dynamic viscosity
ν: Poisson's ratio
$\bar{\nu}$: kinematic viscosity
ϵ: emissivity
$\bar{\sigma}$: Stefan-Boltzmann's constant
ϕ: stress function
χ: holye stress function
$\sigma_{rr}, \sigma_{\theta\theta}, \sigma_{zz}$: normal stress components in cylindrical coords.
σ_{rz}: Shearing-stress component in cylindrical coords.

*1 정회원, 고려대학교 기계공학과

σ_T; thermocapillary coefficient

subscripts
a; actual
max; maximum
∞; ambient

1. Introduction

Since heat and mass transfer during crystal growth influences degree of purification, homogeneity and perfection of a single crystal, much attention has been given on the transport phenomena that occur during the growth of crystals[1,2]. CdTe (Cadmium Telluride) is well known to be an important chemical compound material to detect X-ray and γ-ray and an alternative material of Si and Ge for radiation detectors and infra-red sensors.

Floating-zone crystal growth method is a containless technique which purifies crystals and alloys. Since it is possible to eliminate contaminants from a crucible material, a floating-zone growth technique has been widely adopted since 1950's. A feed rod is pulled and melted through a high temperature zone and the melt resolidifies into a crystal of higher quality.

It is found that natural and thermocapillary convection are the most important flows in a floating-zone crystal growth. Since surface tension depends on temperature, a temperature gradient along the free surface causes the local variation of driving surface tension force and results in bulk flow due to viscosity. The numerical studies in the floating-zone configuration were carried out by many investigators [3,4]. This flow becomes time dependent under certain conditions and much research has been experimentally performed to figure out these phenomena [5,6,7].

During the growth of crystals from the melt, the nonuniform temperature distribution creates thermal stresses in the crystallized ingot. It is one of the main reasons for the appearance of dislocation density, which defects an in-shaped crystal. A great number of papers have been devoted to calculating the thermoelastic stresses that arise in a crystal during other growth processes [8,9,10] rather than the one during floating-zone growth process.

With an advent of spacecraft, utilization of low gravity environment gives much benefits, such as elimination of the effects of gravity or natural convection, in the floating-zone technique. Under microgravity environment, a larger crystal with lower dislocation densities is expected because there is no deformation due to gravity. For this reason the flow and thermal behavior in a floating-zone growth of a crystal under microgravity environment, which is truly believed to become the next generation technique, is studied and the thermal stresses of the resolidified crystal is calculated. In this study thermal stress field rather than the flow and thermal field is investigated in detail.

2. Mathmatical Formulation

A mathematical model of thermocapillary convection with thermal radiation heating mode, i.e., heat flux heating mode, is developed to investigate the flow, temperature and stress field under microgravity environment.

Calculation domain is divided into three parts; feed, melt and crystal part. Each of them are repeatedly computed with separating and matching computational procedures at the co-interface. In this study the object material is considered to be an isotropic material for understanding of heat and mass transfer behavior. Fig. 1 shows the basic characteristics of the simulation process and the heat input profile.

2.1 Momentum, Heat and Mass Transfer

Feed and crystal parts are considered to be a conduction model and a melt part to be a thermocapillary convection model with proper initial and boundary conditions. The calculation procedure of momentum, heat and

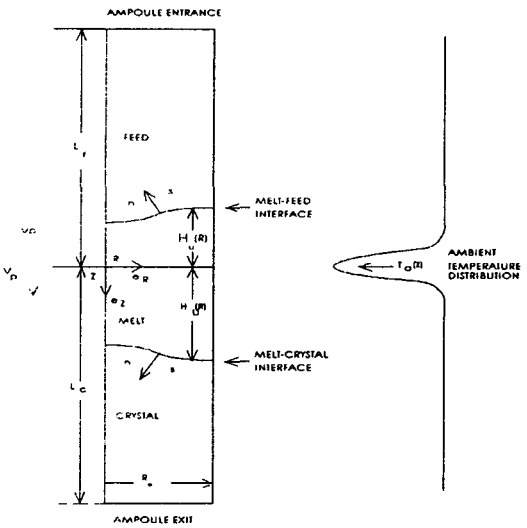

Fig. 1 A basic schematics of a simulation configuration

mass transfer is followed to that by Zheng [3]. The equations are normalized and important parameters are surface tension Reynolds ($Re_\sigma = \sigma_T \Delta T R_0/\mu\bar{\nu}$), Marangoni ($Ma = \sigma_T \Delta T R_0/\mu\bar{\alpha}$), pulling Peclet ($Pe = V_p R_0/\bar{\alpha}$), Stefan ($St = \Delta H/C_p \Delta T$) and radiation ($Ra = \varepsilon\bar{\sigma} T_0^4 R_0/k\Delta T$) numbers. The effect of latent heat is considered at the interface of the phase change. A body-fitted curvilinear coordinate system and finite difference method with stream function-vorticity formulation are employed to estimate the interface shape and transport phenomena in the melt and the crystal.

2.2 Thermal Stresses

In order to obtain the thermal stresses of the crystal part, temperature distribution is calculated in the crystal, especially near the crystal-melt interface. Based on the assumption that the crystals are elastic and isotropic, thermal stresses in the crystals are computed.

The governing equations are

$$\frac{\partial \sigma_{rr}}{\partial r} + \frac{\partial \sigma_{rz}}{\partial z} + \frac{\sigma_{rr} - \sigma_{\theta\theta}}{r} = 0 \tag{1}$$

$$\frac{\partial \sigma_{rz}}{\partial r} + \frac{\partial \sigma_{zz}}{\partial z} + \frac{\sigma_{rz}}{r} = 0 \tag{2}$$

and boundary conditions are

$$-\sigma_{rz} + \sigma_{rr}\tan\theta = 0$$
$$-\sigma_{zz} + \sigma_{rz}\tan\theta = 0 \quad \text{at interface} \tag{3}$$
$$\sigma = \textit{finite} \qquad \textit{at } r = 0 \tag{4}$$
$$\sigma_{zz} = \sigma_{rz} = 0 \qquad \textit{at } z = L \tag{5}$$
$$\sigma_{rr} = 0 \qquad \textit{at } r = R \tag{6}$$

and let

$$(\lambda + 2G)\Delta - \beta T = -\frac{1-\nu}{r}\frac{\partial \chi}{\partial r} \tag{7}$$

$$2Gr\left(\frac{\partial u}{\partial z} - \frac{\partial w}{\partial r}\right) = -(1-\nu)\frac{\partial \chi}{\partial z} \tag{8}$$

$$\psi = -[(1-\nu)\chi + 2Gru] \tag{9}$$

$$\Delta = \frac{\partial u}{\partial r} + \frac{u}{r} + \frac{\partial w}{\partial z} \tag{10}$$

$$\lambda = \frac{\nu E}{(1+\nu)(1-2\nu)} \tag{11}$$

$$G = \frac{E}{2(1+\nu)} \tag{12}$$

$$\beta = (2G + 3\lambda)\alpha \tag{13}$$

and then, the equations become

$$\frac{\partial^2 \chi}{\partial^2 r} - \frac{1}{r}\frac{\partial \chi}{\partial r} + \frac{\partial^2 \chi}{\partial^2 z} = 0 \tag{14}$$

$$\frac{\partial^2 \psi}{\partial^2 r} - \frac{1}{r}\frac{\partial \psi}{\partial r} + \frac{\partial^2 \psi}{\partial^2 z} = \frac{\partial^2 \chi}{\partial^2 z} - \frac{Ea}{1-\nu} r \frac{\partial T}{\partial r} \tag{15}$$

and

$$\sigma_{rr} = -\frac{EaT}{1-\nu} - \frac{1}{r}\frac{\partial \chi}{\partial r} - \frac{1}{r}\frac{\partial \psi}{\partial r} + \frac{\psi + (1-\nu)\chi}{r^2} \tag{16}$$

$$\sigma_{\theta\theta} = -\frac{EaT}{1-\nu} - \frac{\nu}{r}\frac{\partial \chi}{\partial r} - \frac{\psi + (1-\nu)\chi}{r^2} \tag{17}$$

$$\sigma_{zz} = \frac{1}{r}\frac{\partial \psi}{\partial r} \tag{18}$$

$$\sigma_{rz} = -\frac{1}{r}\frac{\partial \psi}{\partial z} \tag{19}$$

Boundary conditions are

$$\psi = 0 \quad \text{all along the boundary} \tag{20}$$
$$\chi = 0 \quad \text{at } r = 0 \tag{21}$$
$$\frac{\partial \chi}{\partial z} = 0 \quad \text{at } z = L \tag{22}$$
$$\sigma_{rr} = -\frac{EaT}{1-\nu} - \frac{1}{r}\frac{\partial \chi}{\partial r} - \frac{1}{r}\frac{\partial \psi}{\partial r} + \frac{\psi + (1-\nu)\chi}{r^2} = 0 \quad \text{at } r = R \tag{23}$$
$$-r\frac{1}{\tan\theta}\frac{\partial \psi}{\partial r} + \left[-\frac{EaT}{1-\nu}r^2 - r\frac{\partial \chi}{\partial r} - r\frac{\partial \psi}{\partial r} + (1-\nu)\chi\right]\tan\theta = 0 \quad \text{at interface} \tag{24}$$

The properties of CdTe in this study are

Table 1 Thermophysical properties of CdTe

Properties	value (unit)
Density	5.7 g/cm^3
Diffusivity	0.01(s), 0.011(m) cm^2/sec
Dynamic Viscosity	0.023 g/cmsec
Kinematic Viscosity	0.04 cm^2/sec
Emissivity	0.2
Latent Heat	209.2 J/g
Melting Temperature	1365 K
Specific Heat	0.355 J/gK
Surface Tension at the melt temperature	220 dynes/cm,
Thermocapillary Coefficient	-0.15 erg/cm^{2}K
Poisson's ratio	0.407

listed in Table 1 and these values are selected from other references.

3. Results and Discussions

In order to understand the flow and thermal behavior for the various operating conditions during the growth process, numerical simulation is performed and all the cases computed are listed in Table 2. The main operating conditions are the heat flux input and the pulling rate. In Cases 1, 2 and 3 the heat input profile is changed to carry out the sensitivity of the growth to concentration and total heat flux input. Cases 4, 5, and 6 include the pulling rate and correspond to Cases 1, 2 and 3, respectively.

Gaussian distributions are assumed for the ambient temperature along the surface generated by a radiant heat source. A heating profile is shown as follows:

$$T_a(z) = (T_{max} - T_\infty)\exp(-z^2/e^2) + T_\infty \qquad (25)$$

Heating profile is controlled by the change of the maximum ambient temperature (t_{max}) and the heating extent (e) in this study.

Fig. 2 shows streamlines and isotherms in a melt and Fig. 3 shows four different

Table 2 Operating conditions of the floating-zone growth

Operating Conditions	Value	
Maximum Ambient Temperature	1392 °C	Case 1,3,4,6
	1282 °C	Case 2,5
Heating Extent	1.0 cm	Case 1,4
	1.5 cm	Case 2,3,5,6
Pulling Rate	0 cm/sec	Case 1,2,3
	0.0001 cm/sec	Case 4,5,6
Ambient Temperature away from the Heating Zone	892 °C	Case 1,2,3,4,5,6
Rod Diameter	1.0 cm	Case 1,2,3,4,5,6
Rod Length	10.0 cm	Case 1,2,3,4,5,6

iso-stress lines in the top of the crystal with an interfacial shape for Case 1. In both figures, only the physical phenomena in the top half of the crystal is demonstrated because of axisymmetry. From Fig. 2, we can deduce that thermocapillary flow is the dominant flow and influences the interfacial shape and the temperature distribution. According to this flow, thermal stresses in a crystal are generated due to non-uniform temperature. The values in Table 3 are nondimensional values of the thermal stresses (based on $Ea\Delta T/(1-\nu)$) and minus sign indicates compression and positive one tension. From the values, it is understood that the intensity of compression is larger than that of tension and $\sigma_{\theta\theta}$ and σ_{rr} are more important stresses than σ_{zz} and

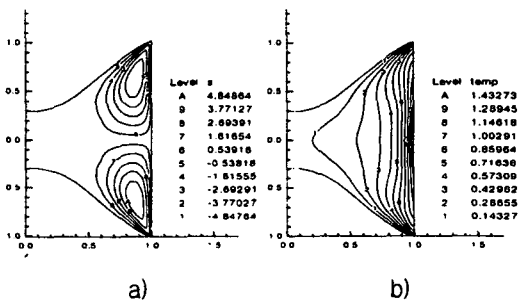

a) b)

Fig. 2 Streamlines and isotherms for case 1
a) Streamlines b) Isotherms

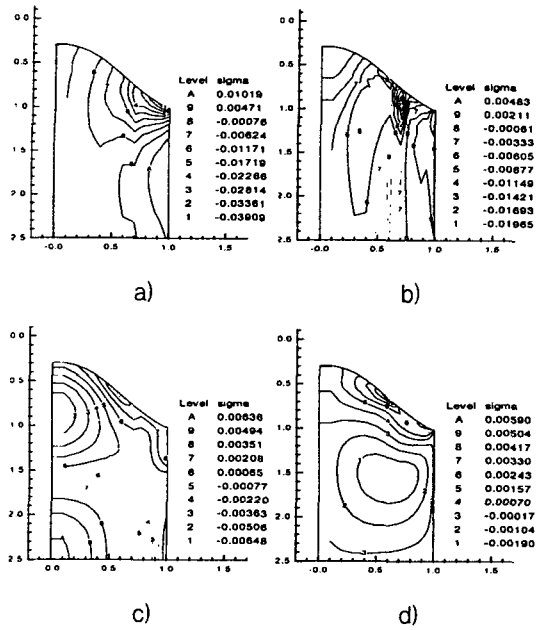

Fig. 3 Four different iso-stress lines for case 1
a) $\sigma_{\theta\theta}$ b) σ_{rr} c) σ_{zz} d) σ_{rz}

σ_{rz}. Accordingly, $\sigma_{\theta\theta}$ has the largest compression. In Fig. 3a, for $\sigma_{\theta\theta}$ near the interface, tension takes place in the region near the axis while going further towards the outer region, compression gets stronger and the maximum value is at a triple point (r=1: a point among melt, crystal, and ambient environment). Compression is generally concentrated at the interface and tension in other regions. As seen in Fig. 3b, σ_{rr} is compression experienced at the entire crystal domain except in the region near the center and the outside boundary. Strong compression is located at the interface of r=0.7. Although σ_{zz} and σ_{rz} have weaker effect than σ_{rr} and $\sigma_{\theta\theta}$, they expand in all regions at the interface and after time passage the stresses change to compression. Therefore, significant compression is located at the interface between the melts and the crystal: roughly σ_{rr} at r=0.7 and $\sigma_{\theta\theta}$ at r=1.0. These stresses create strong crystal dislocations.

Table 3 Computed maximum compression and tension for case 1.

case	stresses	maximum compression	maximum expansion
Case 1	σ_{rr}	-0.02140	0.00658
	$\sigma_{\theta\theta}$	-0.04456	0.01566
	σ_{zz}	-0.00740	0.00728
	σ_{rz}	-0.00246	0.00646

3.1 The Effect of a Radiant Heating Condition

Influences of the various heat flux inputs on the crystal-melt interface is investigated. Increasing /decreasing t_{max} and e expresses the degree of concentration of heating profile and the amount of total heat flux. Total heat flux can be increased with both of them. Fig. 4 presents the interfacial shapes for the various operating conditions (Cases 1 to 6). In sequence of Cases 2 and 3, the total amount of heat input is increased and its profile is diffused compared to Case 1. In Cases 1, 2 and 3 there are interfaces with symmetric shape, while on the other hand, in Cases 4, 5 and 6 there are asymmetric interfacial shapes due to pulling rate. Cases 3 and 6 have larger total heat flux, which have larger melt zones and others have smaller melt zones.

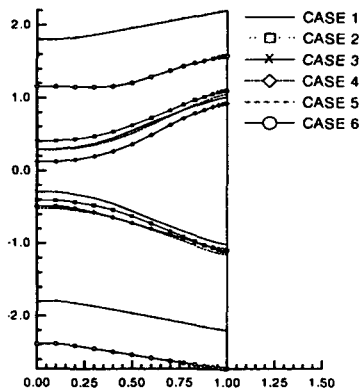

Fig. 4 Calculated interfacial shape for all cases

Table 4 Computed maximum compression and tension for the cases without pulling rate

cases	stresses	maximum compression	maximum expansion
Case 2	σ_{rr}	-0.02450	0.00513
	$\sigma_{\theta\theta}$	-0.03756	0.01104
	σ_{zz}	-0.00617	0.008
	σ_{rz}	-0.00221	0.00588
Case 3	σ_{rr}	-0.02093	0.00744
	$\sigma_{\theta\theta}$	-0.03603	0.01632
	σ_{zz}	-0.00846	0.00758
	σ_{rz}	-0.00267	0.00584

Since the calculated interfacial shapes seem to have almost similar shapes, as shown in Fig. 4, general physical tendency of the flow, thermal and thermal stress field in the cases computed here, are similar to Case 1. Therefore, in this study the graph of the thermal stresses for each case is not presented but just its values are shown in Table 4. In Case 2, where total heat input is slightly increased but diffused against Case 1, it is well shown that the largest tangential compression is reduced. Comparing Cases 2 and 3, only increase of the total heat input gives great influence for the melt size but little influence for the crystal-melt interfacial shape and it does not influence greatly on the behavior of the thermal stresses.

3.2 The Effect of Pulling

The effect of the pulling rate against the interfacial shape and thermal stresses of the crystal is studied. The pulling rate is 0.0001 cm/sec, which is the actual speed rate in crystal growth. Cases 4, 5, and 6 corresponds to Cases 1, 2, and 3, respectively. Comparisons of each value in Table 5 show that the pulling reduces the thermal stresses a bit but due to the slow process nothing significant have changed. Only the pulling effect makes the interfacial shape of the crystal asymmetric and flatter, while thermal stresses become a little weaker.

Table 5 Computed maximum compression and tension for the cases with pulling rate

cases	stresses	maximum compression	maximum expansion
Case 4	σ_{rr}	-0.02061	0.00664
	$\sigma_{\theta\theta}$	-0.04188	0.01571
	σ_{zz}	-0.0076	0.00683
	σ_{rz}	-0.00242	0.00766
Case 5	σ_{rr}	-0.02363	0.0052
	$\sigma_{\theta\theta}$	-0.03694	0.0113
	σ_{zz}	-0.00217	0.00668
	σ_{rz}	-0.00615	0.00729
Case 6	σ_{rr}	-0.02138	0.00828
	$\sigma_{\theta\theta}$	-0.03217	0.01748
	σ_{zz}	-0.00875	0.00779
	σ_{rz}	-0.00362	0.00468

4. Conclusions

The effect of heating condition and the pulling rate on the crystal-melt interfacial shape and thermal stresses of a crystal during the floating-zone crystal growth under microgravity environment are studied.

Thermocapillary convection greatly affects the reformation of a crystal as a dominant convection. From the numerical simulation following conclusions are obtained:

1. Dominant thermal stresses are tangential and radial stresses, $\sigma_{\theta\theta}$ and σ_{rr}.
2. Large values of thermal stresses are concentrated near the crystal-melt interface.
3. Concentrated heating profile increases stresses.
4. Pulling decreases stresses.

Acknowledgements

This work was sponsored by the Korea University Campus Reseach Fund..

References

1. Hurle, D.T.J., and Jakeman, E., "Introduction to the techniques of

crystal growth," Physicochem. Hydrodyn., vol.2 No. 4 (1981), p. 237
2. Pimputkar, S.M. and Ostrach, S., "Convective effects in crystals grown from melt," J. of Crystal Growth, vol. 55 (1981), p. 614
3. Duranceau, J.L. and Brown, R.A., "Thermal-capillary analysis of small-scale floating zones: steady state calculations," J. of Crystal Growth, vol. 75 (1986), p.367
4. Zheng J., "A numerical study of floating zone crystal growth under microgravity," Ph.D. thesis, Dept. of Mech. and Aerospace Engrg., Case Western Reserve Univ. (1990).
5. Chun, C.-H. and Wuest, W., "Experiments on the transition from steady to the oscillatory Marangoni convection of a floating zone under reduced gravity effect," Acta Astronautica, vol.6 (1979), p. 1073
6. Schwabe, D., Velten, R., and Scharmann, A., "The instability of surface tension driven flow in models for floating zones under normal and reduced gravity," J. of Crystal Growth, vol. 99 (1990), p. 1258
7. Lee K.-J., "Experiments on oscillatory thermocapillary flow in simulated floating-zone configurations," Ph.D. thesis, Dept. of Mech. and Aerospace Engrg., Case Western Reserve Univ. (1991)
8. Duseaux, M., "Temperature profile and thermal stress calculations in GaAs crystals growing from the melt," J. of Crystal Growth, vol. 61 (1983), P. 576
9. Meduoye, G.O., Bacon, D.J., and Evans K.E., "The minimisation of thermal stresses during the growth of GaAs crystals," J. of Crystal Growth, vol. 88 (1988), p.397
10. Lambropoulos, J.C., "The isotropic assumption during the Czochralski growth of single semiconductors crystals," J. of Crystal Growth, vol. 84 (1987), p. 349